Smart Sensing for HVAC Control: Collaborative Intelligence in Optical and IR Cameras

Ningyuan Cao, *Member, IEEE*, Justin Ting, *Member, IEEE*, Shreyas Sen, and Arijit Raychowdhury, *Senior Member, IEEE*

***Abstract*—Energy management of heating, ventilation, and cooling (HVAC) has become a primary concern for residential and commercial buildings. In order to save energy without compromising the comfort of occupants, various techniques have been explored to sense the real-time occupancy/vacancy of HVAC zones. Among all these approaches, wireless-camera-based sensing stands out for its potential application in surveillance and security in addition to energy management. However, limited lifetime and detection accuracy have prevented pervasiveness of wireless-camera-based occupancy detection. This paper presents a novel wireless device platform and prototype development that incorporates an infrared (IR) camera with an optical (OP) camera to provide collaborative intelligence at low power and enhanced accuracy. Compared to the single-sensor baseline design, the proposed fusion-based OP/IR design demonstrates $5\times$ miss rate improvement, $5\times$ reduction in false positive rate, and $3\times$ lifetime extension for battery usage with respect to a single-sensor-based design. Compared to a programmed thermostat and schedule-based HVAC control, the design saves a maximum of 26% of HVAC energy.**

***Index Terms*—Data fusion, energy savings, heating, ventilation, and cooling (HVAC) control, occupancy detection.**

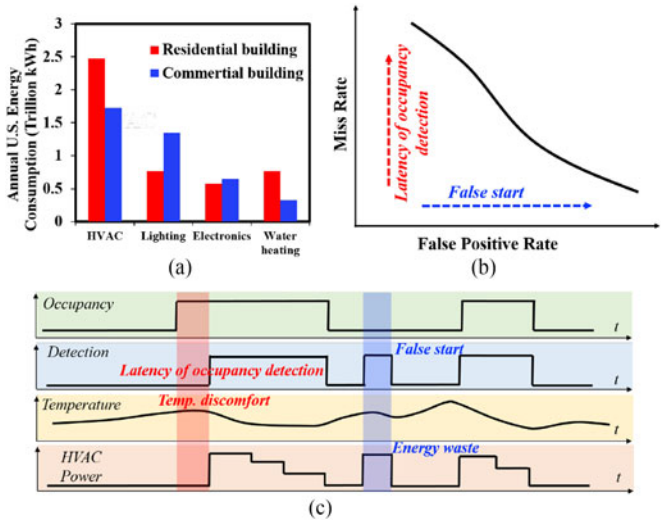

Fig. 1. (a) Residential and commercial energy use [8]. (b) Qualitative assessment of the tradeoff between miss rate and false positive rate. (c) Impact of miss/false positive on latency of occupancy detection/energy waste, respectively.

I. Introduction

HEATING, ventilation, and cooling (HVAC) provides a comfortable climate controlled environment at home and work. However, trillions of kilowatthours of electrical energy are consumed annually in the U.S. [see Fig. 1(a)], which accounts for more than 30% of the energy consumed in all residential and commercial buildings. A total of 10%–40% of this electrical energy is wasted due to inefficiencies, such as unnecessary HVAC operation and overestimated temperature set point. This is further exacerbated by poor and aging insulation on the walls, doors, and windows. To address this challenge, different approaches have been developed. Programmable thermostats, which turn OFF the HVAC system when the house is expected to be vacant, is one common approach for efficient HVAC energy use. However, this approach repeatedly fails at predicting the room occupancy in highly dynamic occupancy pattern [1], [2]. An alternative to a manually programmable schedule based thermostat is the occupancy-based HVAC system, which dynamically senses room occupancy and adaptively controls itself. Among these dynamic detection approaches, radio-frequency identification (RFID) tags [3] and infrared (IR) sensors are popular. RFID tags require humans to wear badges or tags in person, which is an inconvenience and not applicable to residential buildings. IR sensors require motion [4], [5]. On the other hand optical (OP)-camera-based sensors show great potential in occupancy detection [6], [7] even when the occupants are static. However, OP-camera-based occupancy detection remains challenging. They either suffer from high miss rates, resulting in discomfort in the room; or high false positive rates (recognizes a nonhuman object as human) leading to energy wastage in a vacant area. The tradeoff between miss rate and false positive

Manuscript received August 14, 2017; revised December 9, 2017 and February 26, 2018; accepted March 11, 2018. Date of publication March 30, 2018; date of current version July 30, 2018. This work was supported by the Electrical and Computing Department of Georgia Institute of Technology under Grant 2720.001 of Semiconductor Research Corporation. *(Corresponding author: Ningyuan Cao.)*

N. Cao, J. Ting, and A. Raychowdhury are with the School of Electrical and Computer Engineering, Georgia Institute of Technology, Atlanta, GA 30332 USA (e-mail: nycao@gatech.edu; jting31@gatech.edu; arijit.raychowdhury@ece.gatech.edu).

S. Sen is with the School of Electrical and Computer Engineering, Purdue University, West Lafayette, IN 47907 USA (e-mail: shreyas@purdue.edu).

Color versions of one or more of the figures in this paper are available online at http://ieeexplore.ieee.org.

Digital Object Identifier 10.1109/TIE.2018.2818665

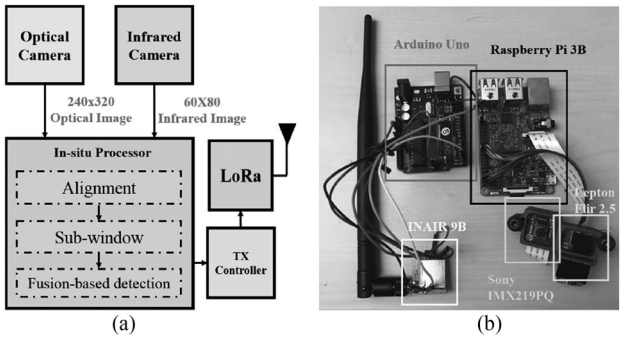

Fig. 2. (a) System architecture of the platform prototype. (b) Hardware setup.

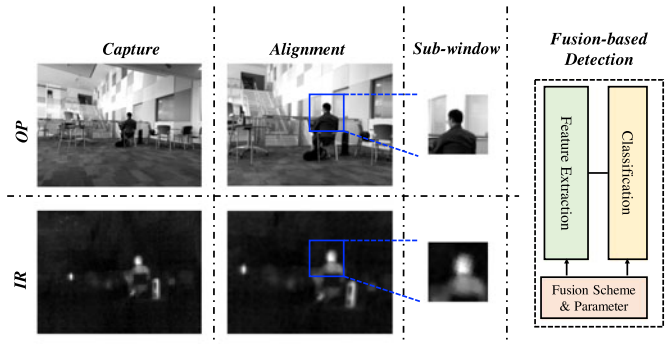

Fig. 3. Demonstration of the algorithm.

rate and their impacts on the occupancy-based HVAC system are illustrated in Fig 1(b) and (c).

To achieve high occupancy detection accuracy, thus improving the occupancy-based HVAC performance, this paper presents a collaborative intelligence solution via data fusion between OP- and IR-camera-based sensor nodes together in a smart wireless sensor network. Collaborative intelligence is achieved *at the sensor node* as well as *among the sensor nodes* at the back-end server, which is located at the HVAC and controls the HVAC. With minimal hardware/software (HW/SW) overhead, the improved detection accuracy results in enhanced comfort, extended sensor lifetime, and reduced HVAC energy wastage.

II. Platform Description

Before going into the algorithmic details, let us discuss the experimental setup. Our prototype sensor comprises an OP camera (IMX219PQ), an IR camera (Flir2.5), an embedded processor for image processing (Raspberry Pi), a long-range radio (LoRa) (INAIR9B), and a transceiver controller (Arduino Uno). The system architecture is shown in Fig. 2(a) and the platform hardware setup is in Fig. 2(b). OP and IR images are captured, aligned, and processed to determine occupancy in the field of view (FoV). The sensed output, including occupancy/vacancy transient or motion vector, is transmitted to the HVAC controller, often at the basement of an office building, using a narrow bandwidth LoRa, which is duty cycled to prevent unnecessary energy expenditure at the sensor. It should be noted that we use LoRa in this paper; however, other communication protocols, such as Wi-Fi can be used in the sensor node. The choice of the communication depends on the available infrastructure, requirements on power, as well as the distance over which the sensor node needs to send necessary signals. This is described in more detail in the following sections.

III. Occupancy Detection via Collaborative Intelligence

Occupancy detection has long been investigated, and different types of special-purpose sensors have been proposed. For example, IR motion sensors, RFID, door sensors, image sensors, etc. Some sensors suffer from low detection rates and some require additional devices to be worn by the occupants to assist detection. In some of these sensors, the occupants need to be in motion, or else the sensor fails to detect occupancy. Most current solutions suffer from low accuracy or longer latency of detection. Our proposed system demonstrates the simultaneous use of both OP and IR cameras. The sensor node fuses the two images, and improves detection rates while minimizing false detection.

Instead of sensing illumination intensity or color as OP cameras do, an IR camera perceives heat emissions. Occupancy detection through IR camera is a promising approach to counter the failures via OP cameras that are caused by darkness, OP foreground/background similarities, and partial occlusion. However, apart from humans, there are other sources that emit IR waves, such as sunlight and machines, which result in false detection for an IR only system. Furthermore, typical (and inexpensive) IR cameras are low of resolution, which prevents efficient machine learning (ML) algorithms to detect features of a human being in the IR domain. Therefore, we combine the advantages of OP and IR detection schemes to provide accurate detection by fusing OP/IR data. The platform captures OP/IR images simultaneously, aligns them by image registration, fuses the information collected from the registered images, and determines the room's occupancy/vacancy from the fused data.

A. Overview

Camera-based occupancy detection, either OP or IR, can be further categorized as video based and image based. A typical video-based detection takes temporal difference [9] between frames, so a successful detection relies on the motion of objects. Therefore, video-based detection will definitely fail for static humans. The image-based approach, in contrast, depends on shapes of objects and is independent of objects' motion. Thus, the proposed system applies image-based detection to handle both moving and motionless objects for realistic residential and commercial building occupancy detection.

After the OP/IR images are captured, the two images are aligned by two-dimensional (2-D) image registration. Then, histogram of oriented gradient (HOG) feature are extracted and classified by an artificial neural network (ANN) template. This algorithm is outlined in Fig. 3.

1) Image Alignment: Accurate alignment of data acquired by sensors with different characteristics is essential in data fusion. In the proposed platform, the FoV and resolutions of OP image sensors and IR image sensors are different. Images captured from the two cameras first need to be registered as a preliminary data-fusion procedure upon deployment to cross-check regions of interest. We assume a long distance between the human and the platform (mounted on the wall near the ceiling), so that any human being can be regarded as 2-D, together with a parallel placement of the OP and IR camera sensors [10]. We apply a rigid translation and the three-dimensional (3-D) translation can, hence, be decomposed into 2-D by

$$\begin{bmatrix} X' \\ Y' \end{bmatrix} = s \begin{bmatrix} \cos\theta & \sin\theta \\ -\sin\theta & \cos\theta \end{bmatrix} \begin{bmatrix} X \\ Y \end{bmatrix} + \begin{bmatrix} \Delta X \\ \Delta Y \end{bmatrix} \tag{1}$$

where a 2-D point (X, Y) in an OP image is transformed to a 2-D point (X', Y') in an IR image with a scaling factor s, rotation angle θ, and offset $(\Delta X, \Delta Y)^{\mathrm{T}}$. Since θ and $(\Delta X, \Delta Y)^{\mathrm{T}}$ are recorded during installation, we only need to perform a calibration to obtain the registration matrix for every image.

2) Feature Extraction: Feature extraction derives informative and nonredundant values to facilitate the subsequent stages to generate better classification results. It is a key stage in performing classification with high accuracy. In human detection, feature extraction is crucial to discriminate human from cluttered background. Different feature descriptors are available, including wavelets, scale-invariant feature transform (SIFT), and HOG. Among all feature extractors, histogram of gradient (HOG) is chosen for its excellent performance [11]–[12]. HOG first divides the input image matrix evenly into $M \times N$ cells. Gradient angle and gradient magnitude of each pixel are computed. Each pixel within the cell votes for an orientation-based histogram channel by comparing gradient angle with angle bins with weight of gradient magnitude. Angle bins evenly spread on $(-\pi, \pi]$ range and the number of bins is N_{bin}. Then, the spatially connected cells form a block of size $(M-1) \times (N-1)$ to be locally normalized to account for changes in illumination and contrast where M and N stand for the number of rows and columns of cells.

3) Classification: Classification is the final step of detection, which takes extracted feature descriptor as an input, compares it with a trained template, and outputs scores indicating the likelihood of a detection (occupied versus unoccupied). Among different classification methods such as support vector machine and Naïve–Bayes tree, a three-layer ANN is selected for its improved performance in classification and linear computation cost [13]. ANN is an information processing paradigm inspired by the biological neural system consisting of input layer, hidden layer, and an output layer. In the current design, the number of input layers is the same as the feature size N_f with hidden and output layers of sizes N_h and N_l, respectively. The output score of the input feature vector is computed as follows:

$$Y(\vec{x}) = \sum_{i=1}^{N_{hl}} \left[\alpha_{\mathrm{i}} \sum_{j=1}^{N_f} (\omega_{ij} x_j + \gamma_{ij}) + \beta_i \right] \tag{2}$$

where x_j is the jth element of the input feature descriptor; and $\omega_{ij}, \gamma_{ij}, \alpha_{\mathrm{i}}$, and β_{i} are the ith hidden neuron weights, biases, output neuron weights, and biases for the jth input element, respectively. In the proposed design, the hidden layer neuron size is fixed to be 100. The computation cost of classification increases with the feature descriptor size. This relation will be discussed in the following section.

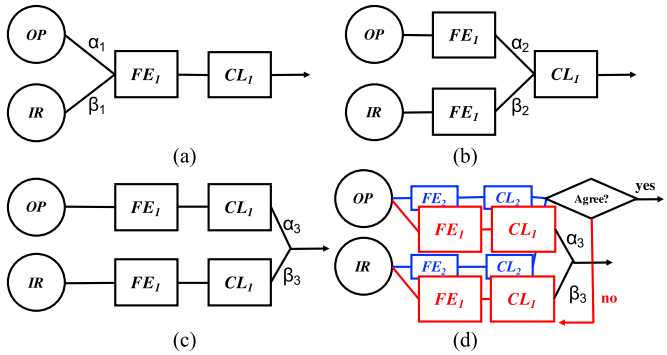

Fig. 4. (a) Data-level fusion; (b) feature-level fusion; (c) decision-level fusion; and (d) the proposed collaborative, hierarchical, and adaptive template (CHAT) algorithm. Here, FE and CL denote feature extraction and classification, respectively.

4) OP/IR Database: With the rapid development of ML technique, a great many OP and IR datasets are generated, such as INRIA, MPII, and InfAR, to facilitate ML-based OP and IR detection/recognition/classification tasks. However, a good "OP+IR" indoor human dataset, where OP and IR images are captured simultaneously targeting fusion-based ML, is still not available to our knowledge. Previous work, such as [14], is only based on limited or separate dataset. This has motivated us to create our own dataset, which (1) contains substantial pairs of positive and negative "OP+IR" pictures and (2) pictures demonstrate diverse OP/IR foregrounds and background features. The collected dataset contains 3727 pairs of 40×40 8-b gray-scale OP/IR images, 1928 positive and 1799 negative, covering foreground samples of humans in different postures and clothing; and background in different lighting conditions and IR intensities. *(The database will be publicly released and is currently not linked for the blind review process.)* Furthermore, to demonstrate realistic results and avoid sample testing, training data and testing data are populated separately with totally different human foreground and OP/IR backgrounds.

B. Fusion-Based Detection

Multisensor data fusion is an emerging technology applied to various areas such as automated target recognition, battlefield surveillance, and autonomous vehicles. It combines data from multiple sensors and related information from the associated databases to achieve improved accuracy that could be achieved by single sensor alone.

A key issue in developing a multisensor data-fusion system is the question of where to accurately combine the data in the data flow. Typical schemes are data-level fusion, feature-level fusion, and decision-level fusion [15], [16], as shown in Fig. 4(a)–(c).

In the proposed occupancy detection system, data-level fusion refers to integrating aligned OP and IR with different weights into a combined single frame, extracting HOG features from

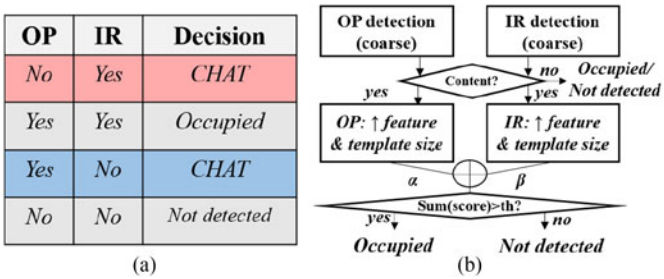

Fig. 5. (a) OP/IR decision table for CHAT. (b) Flow chart of CHAT.

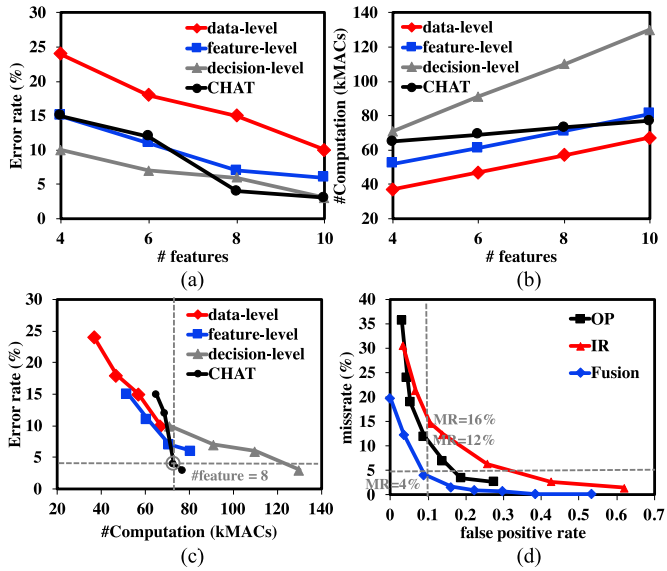

Fig. 6. (a) Error rate versus the number of feature bins. (b) Computation load versus the number of feature bins. (c) Error rate versus computation cost for different fusion scheme. (d) ROC of OP, IR, and "OP+IR" fusion-based detection.

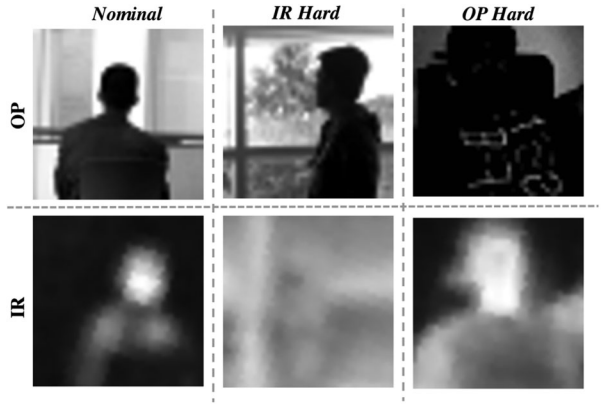

Fig. 7. Prototypical example of nominal, IR hard, and OP hard datasets.

combined data, and classifying the feature with the ANN template. Feature-level fusion refers to extracting HOG feature of OP/IR frames separately and concatenating the weighted two feature descriptors into one single feature descriptor for ANN template inference. Decision-level fusion refers to separate OP/IR frame evaluation and uses the weighted sum of output scores to indicate human occupancy.

Apart from those traditional approaches, this paper presents a novel fusion scheme with CHAT, as is shown in Fig. 4(d). A "coarse" feature descriptor is first extracted for OP and IR images and evaluated by the corresponding "coarse" ANN templates; if two sensors reach consensus, the system outputs the agreed decision, as is shown in Fig. 5(a), otherwise, it goes back and follow a decision-level fusion with "fine-grain" feature extraction and classification, as is shown in Fig. 5(b). The advantages of such an approach are 1) computation cost savings for easy detection environments using the "coarse" feature templates and classification; and 2) accuracy improvement by resolving contentions via hierarchical template adaptation.

To fully explore detection performance and computation cost of the four fusion schemes, experimental results are demonstrated in Fig. 6. As we can observe from Fig. 6(a) and (b), a larger feature space helps us to improve detection accuracy at the cost of increased computation. After feature bin size is equal to or greater than 8, the advantage of CHAT in both detection performance and computation cost becomes apparent. In Fig. 6(c), the maximum accuracy and minimum computation is observed. Based on the above-mentioned measurements, the proposed system selects CHAT as the fusion scheme and all the fusion-based experimental results discussed in the rest of the paper use the CHAT fusion algorithm. The receiver operating characteristic (ROC) of single OP, single IR, and CHAT fusion-based detection schemes in the nominal case are demonstrated in Fig. 6(d). At false positive rate of 0.1, fusion-based detection achieved $3\times$ and $4\times$ miss rate reduction for single OP and IR detection.

C. OP/IR Hard Detection and Sensor Lifetime

Despite the improvement of detection performance in general, a significant benefit of applying fusion-based detection in real environment is that it maintains reasonable detection accuracy when OP and IR sensor alone will fail in extreme cases, and extend the sensor lifetime.

Fig. 7 shows three illustrative cases of data: the nominal case, where both the OP and IR foreground show contrast against the background; the IR hard case, where the IR background is similar to the humans in the foreground; and the OP hard case, where the OP background is similar to the humans in the foreground. In the latter two cases, the corresponding single-sensor system will show heavily degraded performance, more than 50% detection miss at false positive rate (fpr) of 0.1, as is shown in Fig. 8(a) and (b).

As the proposed system is duty cycled to save sensor energy consumption and extend the sensor lifetime, latency of occupancy detection, which is the interval between a person entering the FoV and being detected, depends largely on both the sampling rate and the miss rate for a certain fpr as is shown in Fig. 8(c) and (d). Here, fpr is maintained at 0.1 for both the IR and OP hard cases, and the latency of occupancy detection is reduced at a higher sampling rate. The proposed system

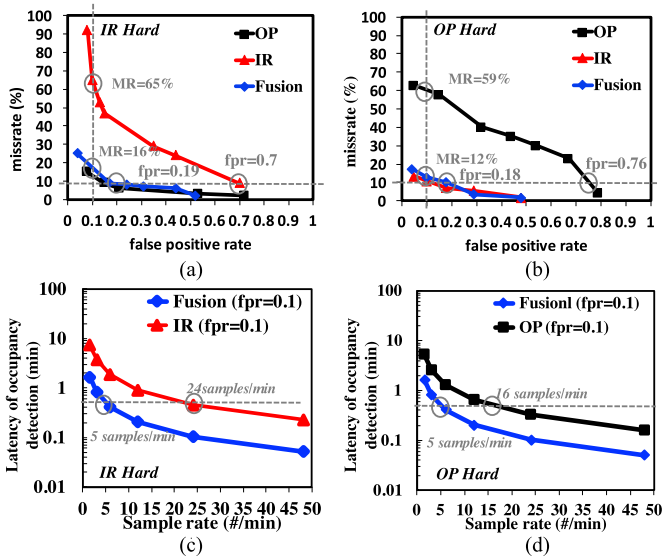

Fig. 8. Measured (a) ROC in IR hard scenario; (b) ROC for OP hard scenario; (c) latency of occupancy detection versus sample rate in IR hard scenario; (d) latency of occupancy detection versus sample rate in OP hard scenario.

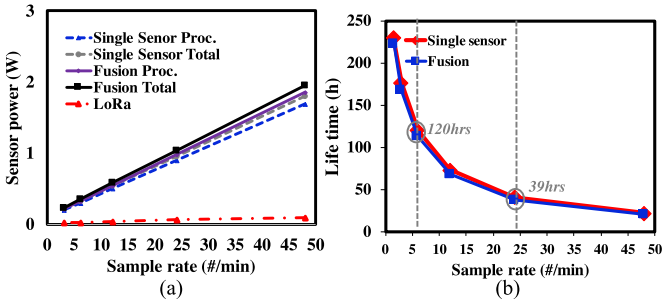

Fig. 9. Measured (a) sensor power consumption versus sample rate, including processing power, LoRa, and total power; (b) sensor lifetime versus sample rate for single and fusion-based sensor.

detects objects more quickly than the corresponding baseline single-sensor designs owing to its lower miss rate. To maintain a maximum target latency of occupancy detection of 30 s, fusion-based sensor platform can sample more slowly and it thus prolongs the sensor lifetime as is shown in Fig. 9, despite the energy overhead brought by an extra sensor.

IV. Smart Sensor Network

In both residential or commercial buildings, more than one sensor is required to cover the whole HVAC zone. These front-end sensors will form a wireless network and periodically transmit sampled data to the back-end HVAC controller. In designing such a network, the maximum number of nodes, maximum range of the network, average sensor power/energy, as well as system-level detection performance are primary concerns. In the proposed system, the intelligence of the front-end sensor is complemented with a network level interdependent wake-up mechanism which optimizes the target design metrics. In this paper, we use LoRa as the communication protocol. However,

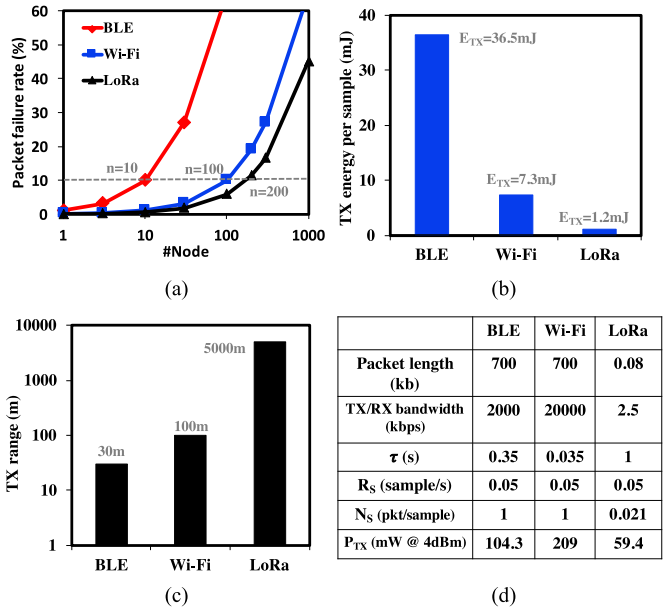

	BLE	Wi-Fi	LoRa
Packet length (kb)	700	700	0.08
TX/RX bandwidth (kbps)	2000	20000	2.5
τ (s)	0.35	0.035	1
R_S (sample/s)	0.05	0.05	0.05
N_S (pkt/sample)	1	1	0.021
P_{TX} (mW @ 4dBm)	104.3	209	59.4

(d)

Fig. 10. Estimated (a) packet failure rate versus the number of nodes in a wireless network for BLE, Wi-Fi, and LoRa, respectively; (b) transmission energy consumption per sample; (c) transmission range; (d) parameter table.

other protocols such as Wi-Fi can be used as well depending on the availability.

A. Intelligent LoRa Front End

In conventional wireless sensor networks, front-end sensors usually follow a centralized "sense-transmit" working scheme: raw data are captured and transmitted directly to the back-end data-center without any *in situ* intelligence. However, for camera-based data-intensive application, such communication strategy not only results in high communication energy and hence low battery life of the sensor node, but also network congestion producing severe quality of service degradation in the form of queueing delay at best, and packet loss or blocking of new connections in the worst case [17]–[20].

To address these issues, the proposed system is equipped with in-sensor data processing capability and notifies the back-end controller (located at the HVAC control) when an area is occupied through low-bandwidth/low-power LoRa. Here, we numerically compare wireless front end of conventional "sense-transmit (bluetooth low energy [BLE], Wi-Fi)" strategy with the proposed intelligent LoRa wireless scheme.

Packet arrival is modeled as a Poisson process [21] and is compared with "sense-transmit (BLE, Wi-Fi)" whose raw data are always transmitted and processed at the back end. In comparison, decentralized "embedded computation + LoRa" suffer from less packet failures in wireless networks with a large number of nodes, as is shown in Fig. 10(a). For example, at 10% packet failure rate, The maximum number of sensors in LoRa network is 200, much larger than the estimated 10(100) of BLE (Wi-Fi) counterpart. Furthermore, the Wi-Fi network is heavily utilized for data transmission, and its use for HVAC control will further exacerbate the network congestion.

An important factor for wireless network is the average transmission energy per sample for individual sensor front end, estimated as follows:

$$E_{tx} = \frac{p_{tx}\tau}{N_s} \tag{3}$$

where E_{tx} stands for the transmission energy per sample and p_{tx} is the active transmission power. Here, we assume transmission time interval is equal to minimum receiver window τ. From Fig. 10(b), we observe that the LoRa-based sensor consumes the least amount of battery energy in our wireless networks for HVAC control.

Apart from the network capacity and transmission energy, transmission range is also important in controlling large HVAC regions, especially in warehouses, and large office buildings. As is shown in Fig. 10(c), the range of LoRa radios outperforms BLE and Wi-Fi by at least 10×. The system parameters are listed in the table of Fig. 10(d).

As we have seen, the advantage of LoRa is the long range over which communication can happen, which is relevant to large commercial buildings or warehouses. Since the in-sensor processor will reduce the data volume that needs to be transmitted to the back end, a narrow-band protocol such as LoRa is an excellent choice. However, Wi-Fi can also be used if available.

In our current experimental setup, the Raspberry PI includes an integrated Wi-Fi radio. We have also enabled an Aduino-based LoRa radio that interfaces with the Raspberry PI. An added advantage of using LoRa in the current setup is the ability to enable fine-grain power management (turning ON and OFF the radio) through the Arduino board—thereby reducing power. More advanced designs, including application-specific integrated circuits (ASICs) may further improve power management on the radio by enabling fast wake-up and sleep; but it is outside the scope of this paper.

B. Collaborative Dynamic Network Control

When detection accuracy is fixed after the employment of the sensor network, minimizing latency of occupancy detection depends on reducing the sample interval (i.e., the number of OP and IR images captured per second), T. However, a high sampling rate will lead to severe sensor energy expenditure and limited sensor lifetime. And it is also noted that the occupancy of a particular region in a building is dependent on its neighboring regions. For example, consider a typical floor plan of a building with three rooms, A, B, and C. The occupancy of room A is dependent on room B if a door between A and B is available and people can walk from B to A as is shown in Fig. 11(a), and vice versa. This motivates the proposed dynamic HVAC control strategy targeting minimized latency of occupancy detection based on a collaborative scheme among neighboring HVAC sections.

Consider a network of sensors deployed as shown in Fig. 11(a). The sensor node at B estimates the presence of an occupant. If an occupant is detected, then it further tracks the occupant via difference of frames and estimation of the direction of motion. The direction of motion is sent to the back end, which resolves the potential adjoining HVAC areas that can be

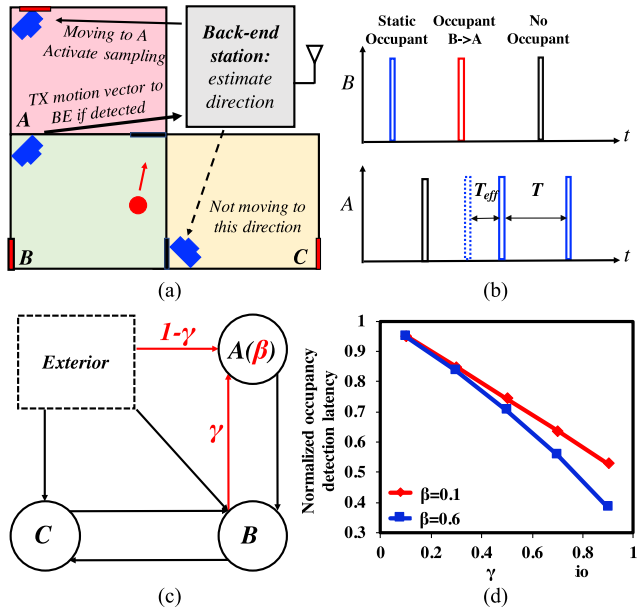

Fig. 11. Illustrative representation of (a) a simple sensor network with interdependence; (b) demonstration of event-driven sampling; (c) network topology; (d) estimated latency of occupancy detection reduced within the collaborative network.

subsequently occupied. In this example, an occupant moving from B toward A will allow the back end to send an "alert" to the sensor node at A. This sensor node, now, increases its sampling rate to reduce the latency of detection. The effective sampling interval T_{eff} is reduced as is shown in Fig. 11(b).

For region A, the occupants are either from outside with no sensor node, or from inside the building, that is monitored by the wireless sensor network. The average effective sampling interval $\overline{T_{\text{eff}}}$ of this region is

$$\overline{T_{\text{eff}}} = \gamma T_{\text{eff}} + (1-\gamma)T \tag{4}$$

where γ represents the ratio of occupants entering A from adjoining rooms to the total number of occupants entering A. This is illustrated in Fig. 11(c). The average sample interval $\overline{T}$ of the sensor node is

$$\overline{T} = \beta\overline{T_{\text{eff}}} + (1-\beta)T \tag{5}$$

where β represents the average occupancy of the region. Although the average sampling rate is temporarily increased, we increase the default sample interval, which enables us to reduce the overall sensor energy. Combining the above-mentioned two equations, we obtain the normalized detection latency

$$d = \frac{2-\gamma}{2-\gamma\beta}. \tag{6}$$

Here, we assume that T_{eff} is $T/2$, the detection latency is proportional to $\overline{T_{\text{eff}}}$ and the sensor lifetime is proportional to $\overline{T}$. The numerical results are demonstrated in Fig. 11(d). Here, we observe that the detection performance is improved significantly, especially in cases of high γ (e.g., $\gamma = 0.8$) and high occupancy β (e.g., $\beta = 0.6$). The corresponding algorithm (implemented at the back end) and a demonstration of the scheme [9], [22] are shown in Fig. 12(a) and (b).

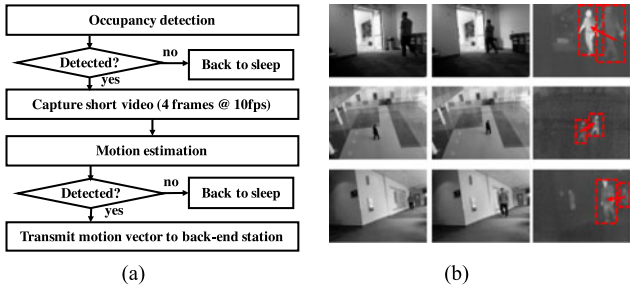

Fig. 12. (a) Flow chart of occupancy/motion detection and sampling rate. (b) Demonstration of a case study.

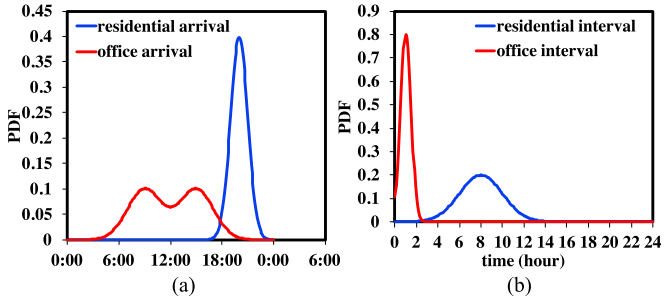

Fig. 13. (a) PDF of arrival time. (b) PDF of time interval between an individual entering and leaving a region.

V. System Measurements

To best evaluate the sensor performance with diverse HVAC systems, two sets of occupancy patterns are randomly generated to simulate an office HVAC environment and a residential HVAC environment. We assume an occupant's arrival time and the duration of stay in a particular HVAC region, follow a normal distribution. In the residential occupant model, the mean arrival time is assumed to be 19:00 in the evening with a standard deviation of 1 h and the mean duration of occupancy of 8 h with a standard deviation of 2 h. For an office occupancy model, on the other hand, we assume that people arrive in the office at 9:00 in morning and leave at 14:00 in afternoon with a standard deviation of 1 h, and leaves the region for a break after 40 min with a standard deviation of 10 min. Occupants' patterns are assumed to be independent and the region is marked as occupied if one or more occupants appear in the region. We assumed that the mean number of occupants is 5 in the residential environment and 40 in an office environment. Fig. 13 shows the probability density function (PDF) of the models and the first subplot of Fig. 14(a) and (b) shows a generated example of residential and office occupancy patterns from the model.

As mentioned in Fig. 6(d), fusion-based detection demonstrates better miss rate/false positive rate tradeoff than single-sensor platforms. When the upper bound of the miss rate is fixed to guarantee a level of human comfort, the proposed fusion-based platform delivers lower false alarm than a single sensor as is shown in the subplots of Fig. 14(a) and (b).

To understand the implication of the sensor-based system on HVAC energy in typical building scenarios, we use EnergyPlus to model the HVAC energy [1] (parameters shown in figure

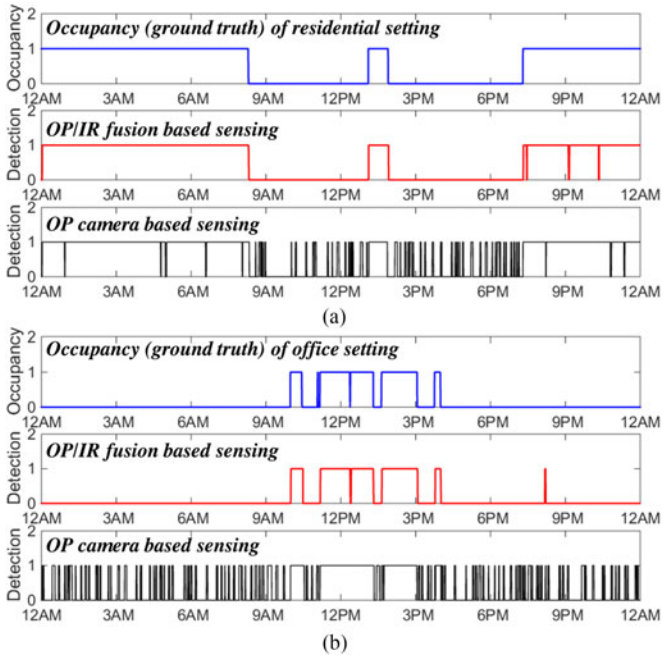

Fig. 14. Simulated system performance showing occupancy (ground truth), fusion-based detection, and single-sensor-based detection in (a) a residential and in (b) an office setting.

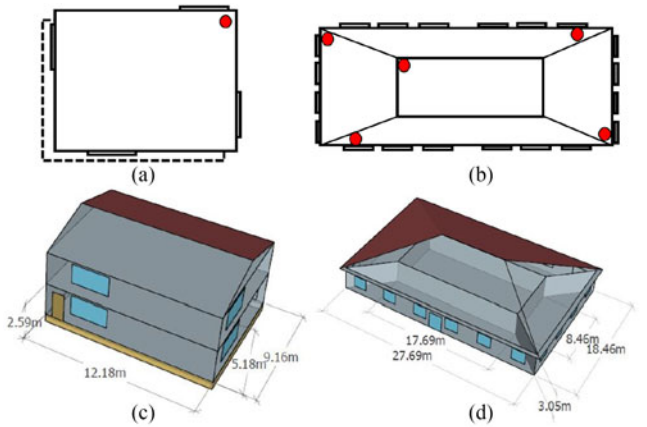

	Total area/m²	Interior volume/m³	# HVAC Zone	Insulation (ft²·°F·h/Btu)		
				Ext Wall	Roof	Floor
Residential	223	578	1	16.4	3.13	1.29
Commercial	511	1559	5	3.45	0.98	2.59

(e)

Fig. 15. HVAC zone floor plan and sensor placement for (a) residential building (b) and commercial building; corresponding 3-D model and dimension in (c) and (d); table in (e) lists all the model parameters.

caption) and the results are discussed for two locations (Chicago and Atlanta). For the results to be representative, we applied reference models from the Department of Energy for both residential and commercial buildings as is shown in Fig. 15. HVAC control patterns based on the occupancy sensor are generated from Fig. 14 and the HVAC controlled by programmed schedule is set from 17:00 to 9:00 for the residential scenario and from 9:00 to 17:00 for the office scenario. For both

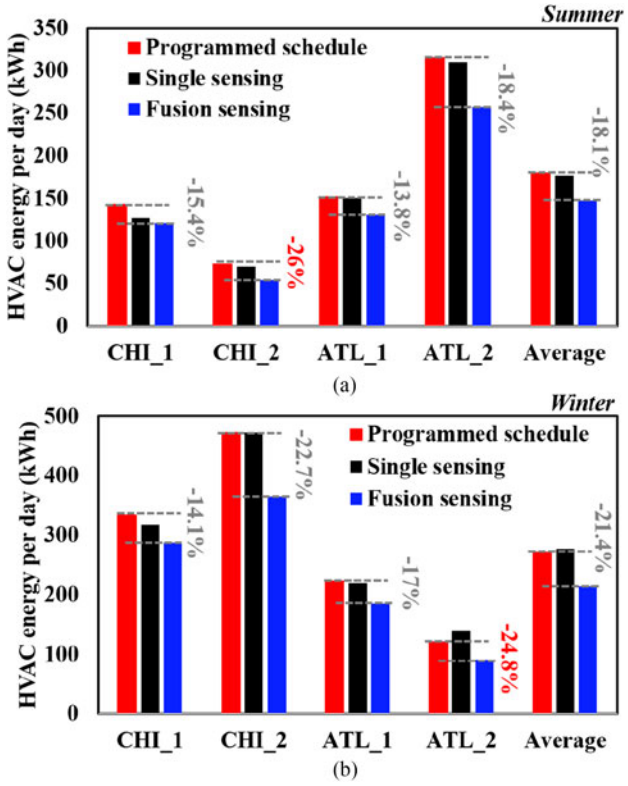

Fig. 16. HVAC energy consumption per day in (a) summer and (b) winter. "CHI"/"ATL" stands for Chicago/Atlanta and "_1"/"_2" stands for residential/office.

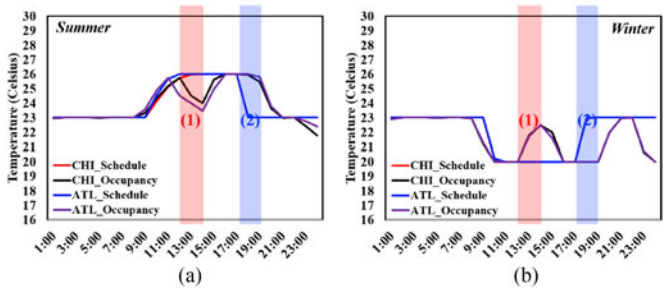

Fig. 17. HVAC region temperature change in (a) summer and (b) winter.

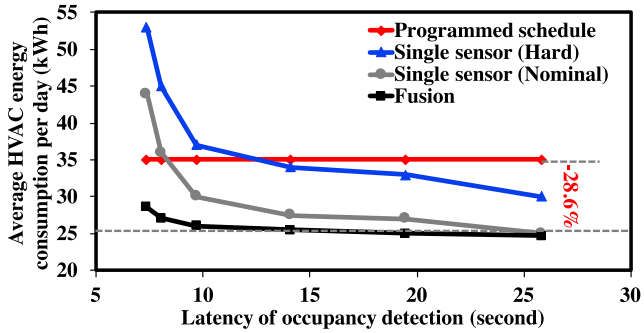

Fig. 18. HVAC energy versus latency of occupancy detection.

	System	Sensor	Accuracy (%)	Energy saving (%)
Motion	[4]	Door+PIR	N.A.	10-15
	[5]	Door+PIR	88	28
	[28]	Camera	80	42
Accessories	[3]	RFID	88/62	N.A.
	[29]	WiFi+phone	86	17.8
Non-intrusive static image	Proposed work	Opical/Infrared Camera	96	13.8-26

Fig. 19. Comparison with existing literature and competing technologies.

sensor-based control and schedule-based control, during summer, the HVAC's hysteretic temperature controls are set to 23 °C and 26 °C; during winter these are set to 23 °C and 20 °C. More advanced control topologies for the HVAC can further reduce HVAC power as described in [23]–[26]. However, the contribution of this paper is the data-fusion in-sensor algorithm and advanced control topologies for control will be left for future work.

Simulation in Fig. 16 shows a maximum of 26% (CHI_2) in summer and an average of 18.1–21.4% energy savings are achieved in the fusion-based sensing compared with a schedule-based HVAC control. With our current model, the HVAC system saves around 30 kWh per day in summer and 55 kWh per day in winter on an average. At the same time, a single-sensor-based platform, due to its high false positive rate, consumes more energy than the schedule-based HVAC control.

In Fig. 17, the indoor temperature change in one day is demonstrated with residential occupancy pattern shown in subplot1 of Fig. 14(a). In both summer and winter, occupancy-based HVAC control outperforms schedule-based control in sampling "unusual" human arrivals, as is shown in the highlighted region where the resident unexpectedly (1) comes back home at noon and stays for a while and (2) arrives home later than usual. In case (1), HVAC is dynamically turned ON to provide comfortable environment and in case (2), HVAC is kept OFF at time of vacancy, which saved HVAC energy.

Fig. 18 shows the tradeoff between the HVAC energy savings and detection latency. We observe that energy is saved for all the sensor-based HVAC when more detection latencies are tolerated. We also note that when we have strict detection latency constraints, a single-sensor-based HVAC control, especially in IR or OP hard cases, performs worse than a simple schedule-based control.

Comparison with the state-of-the-art HVAC occupancy detection platform is demonstrated in the table of Fig. 19. Depending on the mechanism of detecting occupancy, these works are divided into motion-based approach, such as IR and camera [4], [5], [27], accessory-based approach, which includes RFID and smart phone [3], [28], as well as the proposed nonintrusive camera based approach. Our proposed work shows high accuracy and significant energy savings from the HVAC system without being intrusive or relying on motion for occupancy detection.

VI. Conclusion

We proposed a novel collaborative and adaptive template based data-fusion algorithm between an OP and an IR camera, which shows significant improvement in miss rate (5×) and

false positive rate (5×), extends the lifetime of a wireless sensor lifetime by 3×, and achieved a maximum of 26% HVAC energy savings compared to schedule-based control.

Acknowledgment

The authors would like to thank J. Chen from the School of Building Construction, Georgia Institute of Technology, for the kind help and advice on HVAC modeling.

References

[1] J. Lu *et al.*, "The smart thermostat: Using occupancy sensors to save energy in homes," in *Proc. 8th ACM Conf. Embedded Netw. Sensor Syst.*, New York, NY, USA, 2010, pp. 211–224. [Online]. Available: http://doi.acm.org/10.1145/1869983.1870005

[2] T. Peffer, M. Pritoni, A. Meier, C. Aragon, and D. Perry, "How people use thermostats in homes: A review," *Building Environ.*, vol. 46, no. 12, pp. 2529–2541. [Online]. Available: http://www.sciencedirect.com/science/article/pii/S0360132311001739

[3] N. Li, G. Calis, and B. Becerik-Gerber, "Measuring and monitoring occupancy with an RFID based system for demand-driven HVAC operations," *Autom. Construction*, vol. 24, pp. 89–99, Jul. 2012. [Online]. Available: http://www.sciencedirect.com/science/article/pii/S0926580512000283

[4] Y. Agarwal, B. Balaji, R. Gupta, J. Lyles, M. Wei, and T. Weng, "Occupancy-driven energy management for smart building automation," in *Proc. 2nd ACM Workshop Embedded Sens. Syst. Energy-Efficiency Building*, 2010, pp. 1–6. [Online]. Available: http://doi.acm.org/10.1145/1878431.1878433

[5] J. Lu *et al.*, "The smart thermostat: Using occupancy sensors to save energy in homes," in *Proc. 8th ACM Conf. Embedded Netw. Sensor Syst.*, 2010, pp. 211–224. [Online]. Available: http://doi.acm.org/10.1145/1869983.1870005

[6] N. Cao, S. Nasir, S. Sen, and A. Raychowdhury, "In-sensor analytics and energy-aware self-optimization in a wireless sensor node," in *Proc. IEEE Int. Microw. Symp.*, 2017, pp. 200–203.

[7] N. Cao, B. S. Nasir, S. Sen, and A. Raychowdhury, "Self-optimizing IoT wireless video sensor node with in-situ data analytics and context-driven energy-aware real-time adaptation," *IEEE Trans. Circuits Syst. I, Reg. Paper* vol. 64, no. 9, pp. 2470–2480, Sep. 2017. [Online]. Available: http://www.sciencedirect.com/science/article/pii/S0926580512000283

[8] "Buildings overview | Center for Climate and Energy Solutions." 2014. [Online]. Available: https://www.c2es.org/technology/overview/buildings. Accessed: Apr. 5, 2018.

[9] Z. Yi and F. Liangzhong, "Moving object detection based on running average background and temporal difference," in *Proc. IEEE Int. Conf. Intell. Syst. Knowl. Eng.*, Nov. 2010, pp. 270–272.

[10] J. Han and B. Bhanu, "Fusion of color and IR video for moving human detection," *Pattern Recognit.*, vol. 40, no. 6, pp. 1771–1784, Jun. 2007. [Online]. Available: https://www.sciencedirect.com/science/article/pii/S003132030600478X

[11] N. Dalal and B. Triggs, "Histograms of oriented gradients for human detection," in *Proc. IEEE Comput. Soc. Conf. Comput. Vis. Pattern Recognit.*, Jun. 2005, vol. 1, pp. 886–893.

[12] Q. Zhu, M.-C. Yeh, K.-T. Cheng, and S. Avidan, "Fast human detection using a cascade of histograms of oriented gradients," in *Proc. IEEE Comput. Soc. Conf. Comput. Vis. Pattern Recognit.*, 2006, vol. 2, pp. 1491–1498.

[13] S. Dreiseitl and L. Ohno-Machado, "Logistic regression and artificial neural network classification models: A methodology review," *J. Biomed. Informat.*, vol. 35, no. 5, pp. 352–359, Oct. 2002. [Online]. Available: http://www.sciencedirect.com/science/article/pii/S1532046403000340

[14] N. Cao, S. Sen, and A. Raychowdhury, "Collaborative intelligence in optical/IR camera based wireless sensor nodes for HVAC control," in *Proc. IEEE Sensors Conf.*, pp. 1–3, Nov. 2017. [Online]. Available: http://www.sciencedirect.com/science/article/pii/S1532046403000340

[15] D. L. Hall and J. Llinas, "An introduction to multisensor data fusion," in *Proc. IEEE*, vol. 85, no. 1, pp. 6–23, Jan. 1997.

[16] B. Khaleghi, A. Khamis, F. O. Karray, and S. N. Razavi, "Multisensor data fusion: A review of the state-of-the-art," *Inf. Fusion*, vol. 14, no. 1, pp. 28–44, Jan. 2013. [Online]. Available: http://www.sciencedirect.com/science/article/pii/S1566253511000558

[17] J. Yick, B. Mukherjee, and D. Ghosal, "Wireless sensor network," *Comput. Netw.*, vol. 52, no. 12, pp. 2292–2330, Aug. 2008. [Online]. Available: http://dx.doi.org/10.1016/j.comnet.2008.04.002

[18] F. Ren, T. He, S. K. Das, and C. Lin, "Traffic-aware dynamic to alleviate congestion in wireless sensor networks," *IEEE Trans. Parallel Distrib. Syst.*, vol. 22, no. 9, pp. 1585–1599, Sep. 2011.

[19] C.-Y. Wan, S. B. Eisenman, and A. T. Campbell, "CODA: Congestion detection and avoidance in sensor networks," in *Proc. 1st Int. Conf. Embedded Netw. Sensor Syst.*, New York, NY, USA, 2003, pp. 266–279. [Online]. Available: http://doi.acm.org/10.1145/958491.958523

[20] T. Pal, S. Bandyopadhyay, and S. Dasbit, "Energy-saving image transmission over WMSN using block size reduction technique," in *Proc. IEEE Int. Symp. Nanoelectron. Inf. Syst.*, Dec. 2015, pp. 41–46.

[21] H. C. Tijms, *A First Course in Stochastic Models*. Hoboken, NJ, USA: Wiley, May 2003.

[22] M. K. Chowdary, S. S. Babu, S. S. Babu, and H. Khan, "FPGA implementation of moving object detection in frames by using background subtraction algorithm," in *Proc. Int. Conf. Commun. Signal Process.*, Apr. 2013, pp. 1032–1036.

[23] S. Soyguder, M. Karakose, and H. Alli, "Design and simulation of self-tuning PID-type fuzzy adaptive control for an expert HVAC system," *Expert Syst. Appl.*, vol. 36, no. 3, pp. 4566–4573. [Online]. Available: http://www.sciencedirect.com/science/article/pii/S0957417408002200

[24] S. Soyguder and H. Alli, "An expert system for the humidity and temperature control in HVAC systems using ANFIS and optimization with fuzzy modeling approach," *Energy Buildings*, vol. 41, no. 8, pp. 814–822. [Online]. Available: http://www.sciencedirect.com/science/article/pii/S0378778809000486

[25] S. Soyguder and H. Alli, "Predicting of fan speed for energy saving in HVAC system based on adaptive network based fuzzy inference system," *Expert Syst. Appl.*, vol. 36, no. 4, pp. 8631–8638. [Online]. Available: http://www.sciencedirect.com/science/article/pii/S0957417408007288

[26] S. Soyguder, "Intelligent system based on wavelet decomposition and neural network for predicting of fan speed for energy saving in HVAC system," *Energy Buildings*, vol. 43, no. 4, pp. 814–822. [Online]. Available: http://www.sciencedirect.com/science/article/pii/S0378778810004214

[27] V. L. Erickson, M. A. Carreira, and A. E. Cerpa, "Observe: Occupancy-based system for efficient reduction of HVAC energy," in *Proc. 10th ACM/IEEE Int. Conf. Inf. Process. Sensor Netw.*, 2011, pp. 258–269.

[28] B. Balaji, J. Xu, A. Nwokafor, R. Gupta, and Y. Agarwal, "Sentinel: Occupancy based HVAC actuation using existing wifi infrastructure within commercial buildings," in *Proc. 11th ACM Conf. Embedded Netw. Sensor Syst.*, 2013, Art. no. 17. [Online]. Available: http://doi.acm.org/10.1145/2517351.2517370

Ningyuan Cao (M'17) received the B.S. degree from Shanghai Jiaotong University, Shanghai, China, and the M.S. degree from Columbia University, New York, NY, USA, both in electrical engineering, in 2013 and 2015, respectively. He is currently working toward the Ph.D. degree in electrical engineering with Georgia Institute of Technology, Atlanta, GA, USA.

Since 2015, he has been with the Integrated Circuit and System Research Lab, Georgia Institute of Technology. His research interests include low-power machine learning ASIC design, wireless sensor design, power management, and energy harvesting circuit design.

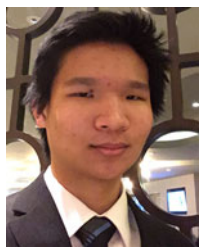

Justin Ting (M'18) is currently working toward the B.S. degree major in electrical engineering, as well as a dual minor in music and computer science theory at Georgia Tech, Atlanta, GA, USA.

In the spring of 2017, he was involved in the Vertically Integrated Projects hardware security team, where he worked on configuring an Field-programmable Gate Array (FPGA) to securely boot a microcontroller. He joined ICSRL during the summer of 2017. His current research focuses on implementing neural networks onto FPGAs, as well as FPGA control over robotic motion.

Shreyas Sen (S'06–M'11) received the Ph.D. degree in electrical and computer engineering from Georgia Tech, Atlanta, GA, USA, in 2011.

He is currently an Assistant Professor with the School of Electrical and Computer Engineering, Purdue University, West Lafayette, IN, USA. He has more than five years of industry experience as a Research Scientist with Circuit Research Lab and Wireless Communication Research, Intel Labs and as a Research Intern with Qualcomm and Rambus. He has authored/coauthored two book chapters, more than 100 journal and conference papers, and has 13 patents granted/pending. His research interests include mixed-signal circuits/systems for Internet of Things, biomedical, and security.

Dr. Sen was the recipient of the MIT TR35 India Award 2018, NSF CISE CRII Award 2017, AFOSR Young Investigator Award 2017, Google Faculty Research Award 2017, Intel Labs Divisional Recognition Award 2014 for industry-wide impact on USB-C type, Intel Ph.D. Fellowship 2010, IEEE Microwave Fellowship 2008, GSRC Margarida Jacome Best Research Award 2007, HOST Best Student Paper Award 2017, ICCAD Best-in-Track Award 2014, VTS Honorable Mention Award 2014, RWS Best Paper Award 2008, Intel Labs Quality Award 2012, SRC Inventor Recognition Award 2008, and Young Engineering Fellowship in 2005. He serves/has served as an Associate Editor for the IEEE DESIGN & TEST, the Executive Committee member of the IEEE Central Indiana Section, ETS, and the Technical Program Committee member of DAC, DATE, ICCAD, ITC, VLSI Design, IMSTW, and VDAT.

Arijit Raychowdhury (M'07–SM'13) received the Ph.D. degree in electrical and computer engineering from Purdue University, West Lafayette, IN, USA, in 2007.

He joined Georgia Tech in 2013 and is currently an Associate Professor with the School of Electrical and Computer Engineering, Georgia Institute of Technology (Georgia Tech), Atlanta, GA, USA, where he currently holds the ON Semiconductor Junior Professorship. His industry experience includes five years as a Staff Scientist with the Circuits Research Lab, Intel Corporation, and a year as an Analog Circuit Researcher with Texas Instruments, Inc. He holds more than 25 U.S. and international patents and has authored or coauthored more than 100 articles in journals and refereed conferences. His research interests include low-power digital and mixed-signal circuit design, device-circuit interactions, and novel computing models and hardware realizations.

Dr. Raychowdhury was the recipient of the Intel Early Faculty Award, 2015; NSF CISE Research Initiation Initiative Award, 2015; Intel Labs Technical Contribution Award, 2011; Dimitris N. Chorafas Award for outstanding doctoral research, 2007; the Best Thesis Award, College of Engineering, Purdue University, 2007; and multiple best paper awards and fellowships.